Data in Brief 57 (2024) 110919

Contents lists available at ScienceDirect

Data in Brief

journal homepage: www.elsevier.com/locate/dib

Data Article

Data of crystal structure of the large Stokes shift fluorescent protein tKeima

Ki Hyun Nam [a,*], Yongbin Xu [b,c]

[a] College of General Education, Kookmin University, Seoul 02707, Republic of Korea
[b] Department of Bioengineering, College of Life Science, Dalian Minzu University, Dalian 116600, China
[c] Key Laboratory of Biotechnology and Bioresources Utilization of Ministry of Education, College of Life Science, Dalian Minzu University, Dalian 116600, China

ARTICLE INFO

Article history:
Received 5 August 2024
Revised 30 August 2024
Accepted 2 September 2024
Available online 7 September 2024

Dataset link: Crystal structure of large stokes shift red fluorescent protein tKeima (Original data)

Keywords:
tKeima
Fluorescent protein
Large stroke shift
X-ray diffraction
Crystal structure

ABSTRACT

Large Stokes shift (LSS) fluorescent proteins (FPs) are important for dual-color fluorescence cross-correlation spectroscopy and multicolor imaging. tKeima is a tetrameric LSS FP from the stony coral *Montipora* sp. Analyzing the tetrameric interface of tKeima is necessary to understand the oligomeric state of the Keima family and to provide insights into engineering oligomeric FPs to generate monomeric FPs, which are useful for FP-based molecular and cell biology studies. Here, detailed experimental procedures for tKeima were reported, including spontaneous crystal growth, data collection for X-ray diffraction, and structure determination. This information can be used for future experiments to obtain the high-resolution structure of tKeima, providing accurate structural information to comprehensively understand the molecular function of tKeima and the protein engineering of tetrameric FPs.

* Corresponding author.
E-mail address: structure@kookmin.ac.kr (K.H. Nam).

https://doi.org/10.1016/j.dib.2024.110919

Specifications Table

Subject	Biological science
Specific subject area	Structural Biology
Type of data	Processed
Data collection	Synchrotron: Pohang Light Source II (PLS-II) Beamline: 11C Detector: Pilatus 6M (DECTRIS) Data collection temperature: 100 K Data processing program: HKL2000
Data source location	Institution: Kookmin University City/Town/Region: Seoul Country: Republic of Korea
Data accessibility	Structure factor and coordinates Repository name: Protein Data Bank Data identification number: https://doi.org/10.2210/pdb8XC6/pdb Direct URL to data: https://www.rcsb.org/structure/8XC6 Instructions for accessing these data: Coordinate and structure factor can be download without permission
Related research article	K.H. Nam, Y. Xu, Structural Analysis of the Large Stokes Shift Red Fluorescent Protein tKeima, Molecules 29(11) (2024) 2579. https://doi.org/10.3390/molecules29112579 [1]

1. Value of the Data

- Purified tKeima was spontaneously crystallized without performing crystallization.
- These data provide the coordinates and structure factors for analyzing the crystal structure of tKeima.
- These data provide information on the X-ray diffraction data and model structure for evaluating the quality of the tKeima structure.
- These data provide detailed information on the interface interactions in tetrameric tKeima, explaining how the tKeima tetramer formation is stabilized.
- The tKeima structure provides insights into the generation of novel monomeric fluorescent proteins.

2. Background

Fluorescent proteins (FPs) are widely used as optical probes in molecular and cell biology studies, as well as in biosensor research [2–6]. Large Stoke shift (LSS) FPs can be applied to multicolor imaging experiments, two-photon laser scanning microscopy, dual-color fluorescence cross-correlation spectroscopy for quantifying protein–protein interactions, fluorescence resonance energy transfer (FRET), and multicolor imaging [7–9]. tKeima is a tetrameric LSS FP in which monomeric and dimeric Keima proteins are originated [8]. With regard to biological applications, monomeric FPs are preferred to avoid slow maturation and to improve FRET applications [10]. Structural analysis of tKeima can provide comprehensive understanding of its unique spectral properties and insights into protein engineering to generate efficient monomeric FPs. In this study, the detailed process of data collection and structure determination was reported to provide further information on the protein engineering of tKeima.

3. Data Description

Codon-optimized tKeima was overexpressed in *E. coli* and purified using Ni-NTA purification and gel filtration chromatography. The purified tKeima solution was concentrated and incubated at 4 °C for crystallization. The next day, the concentrated purified tKeima proteins were spontaneously crystallized in microtubes (Fig. 1A). The size of tKeima crystals varied between 10

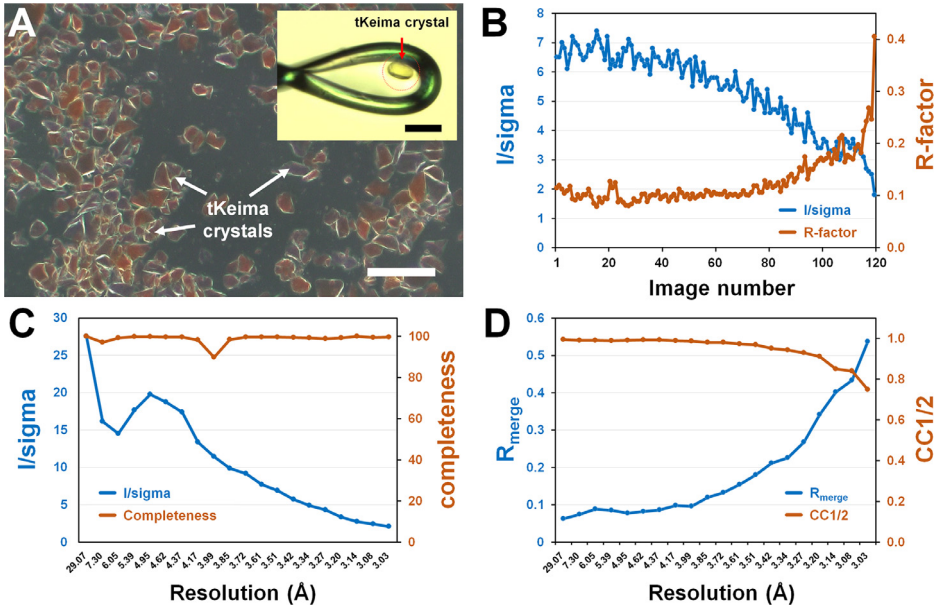

Fig. 1. Spontaneously grown tKeima crystals and processing statistics of XRD data. (A) Photo of spontaneously grown tKeima crystals. (Inset) tKeima crystal used for XRD data collection. The original photo was obtained from [1] and modified. (B) Plot of I/sigma and R-factor for tKeima XRD images. (C) Data processing plot of tKeima for I/sigma and completeness. (D) Data processing plot of tKeima for R_{merge} and CC1/2.

and 50 μm, with most crystals being irregularly shaped. Most irregularly shaped tKeima crystals showed poor diffraction, making them unsuitable for determining the crystal structure. Meanwhile, a rhombic-shaped tKeima crystal (20 μm × 20 μm × 40 μm, Fig. 1A), which was rarely observed in the crystal suspension, was considered suitable for diffraction data collection. This crystal was cryoprotected, and X-ray diffraction data were collected at beamline 11C at Pohang Light Source II (PLS-II). A total of 120 diffraction images were processed up to a 3.0 Å resolution. The indexing results of diffraction images indicated that the tKeima crystal belongs to the orthorhombic space group $P22_12_1$ with unit cell dimensions of a = 69.88 Å, b = 83.50 Å, and c = 109.78 Å. The diffraction data were processed in the resolution range of 50–3.0 Å, with a total of 13,250 reflections. The overall completeness, I/sigma, R_{merge}, and CC1/2 were 98.9, 5.4, 0.119, and 0.995, respectively (Table 1).

The average I/sigma and R_{merge} from the initial 10 images were 6.72 and 0.1054, respectively, whereas the average I/sigma and R_{merge} from the last 10 images were 2.97 and 0.2296, respectively (Fig. 1B). These results indicate that the diffraction quality of the tKeima crystal decreased with the increase X-ray exposure. The completeness of the tKeima diffraction data was greater than 97 % for all processed resolutions, except in the range of 4.07–3.91 Å, where the completeness was 89.9 % (Fig. 1C). The I/sigma values at the low-resolution and high-resolution regions were approximately 27.5 and 2.07, respectively (Fig. 1C). The R_{merge} value was less than 0.3 at resolutions below 3.23 Å, whereas the R_{merge} value was 0.543 at the region with the highest resolution (Fig. 1D). The CC1/2 value of the tKeima diffraction data was greater than 0.97 at resolutions ranging from 50 to 3.17 Å, whereas that at the highest resolution was 0.75 (Fig. 1D).

Two tKeima molecules occupy the asymmetric unit, with a Matthews coefficient (Vm) of 3.20 $Å^3$/Dalton and an estimated solvent content of 61.52 %. The final model was refined to 3.0 Å resolution, with R_{work} and R_{free} values of 19.6 % and 24.7 %, respectively (Table 2).

Table 1
Data collection statistics for tKeima. Processing statistics have been presented elsewhere [1].

Data collection	tKeima
X-ray Source	11C beamline, PLS-II
Wavelength (Å)	0.9794
Space group	$P22_12_1$
Cell dimension	
a, b, c (Å)	69.88, 83.50, 109.78
α, β, γ (°)	90.0, 90.0, 90.0
Resolution (Å)	50.0–3.00 (3.05–3.00)
Unique reflections	13,250 (649)
Completeness (%)	98.9 (99.7)
Redundancy	4.3 (4.6)
$I/\sigma(I)$	10.9 (2.1)
R_{merge}	0.119 (0.537)
CC1/2	0.981 (0.750)
CC*	0.995 (0.926)

Values for the outer shell are given in parentheses.

Table 2
Refinement statistics for tKeima. Refinement statistics have been presented elsewhere [1].

Refinement	tKeima
Resolution (Å)	48.21–3.00
R_{work} [a]	0.196
R_{free} [b]	0.247
R.m.s. deviations	
Bonds (Å)	0.007
Angles (°)	1.451
B factors (Å^2)	
Protein	53.45
Chromophore	72.80
Ramachandran plot	
Favored (%)	95.18
Allowed (%)	4.13

Values for the outer shell are given in parentheses. [a] $R_{work} = \Sigma||F_{obs}| \Sigma |F_{calc}||/\Sigma|F_{obs}|$, where F_{obs} and F_{calc} are the observed and calculated structure factor amplitudes, respectively. [b] R_{free} was calculated as R_{work} using a randomly selected subset of unique reflections not used for structural refinement.

The electron density maps of tKeima were well defined for all amino acids (Met1-Gly222) and for the three N-terminal amino acids (Ser–His–Met) from the expression tag. Geometry analysis showed that most of the amino acids were located in the favored (95.18 %) and allowed (4.13 %) regions of the Ramachandran plot (Fig. 2). Meanwhile, the amino acids Pro127 (φ, ψ: −29.2, 124.8) from Molecule A and Met0 (−64.1, 82.7) and Lys182 (162.8, 118.3) from Molecule B were located in the outlier regions.

The tKeima monomer structure exhibited a typical β-barrel fold, with a chromophore consisting of the tripeptide Gln63-Tyr64-Gly65, which showed *p*-hydroxybenzylidineimidazolinone through posttranslational modification (Fig. 3A). The electron density map of the two tKeima chromophores from the asymmetric unit primarily showed a cis-conformation between the tyrosine and imidazoline rings (Fig. 3A). The tKeima chromophore interacts with Tyr11 (3.26 Å: average distance from two tKeima molecules in the asymmetric unit), Ser143 (2.98 Å), and Gln210 (3.18 Å). The tyrosine ring is surrounded by Pro60, Met160, Phe174, Arg194, and Leu196 residues at distances of 4.33, 3.24, 4.55, 3.46, and 3.42 Å, respectively (Fig. 3B).

The crystal packing of tKeima with 222 symmetry exhibited a tetramer formation (Fig. 4A), which is consistent with the tetrameric state observed in solution by gel filtration chromatog-

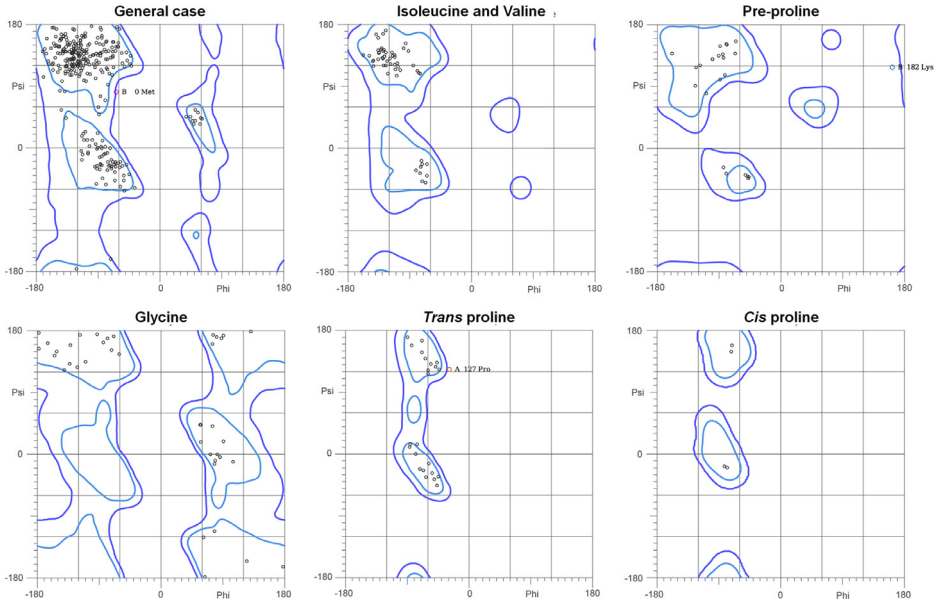

Fig. 2. Ramachandran plot of the final model structure of tKeima.

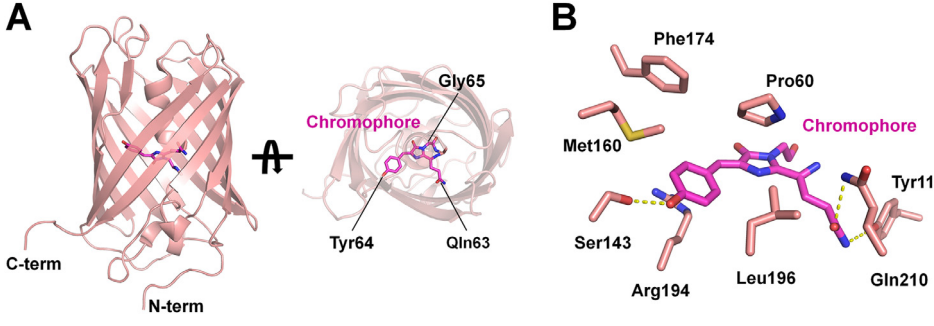

Fig. 3. Crystal structure of tKeima. (A) Monomeric structure of tKeima comprising the chromophore with cis-conformation. (B) Interaction of the tKeima chromophore with amino acids in its vicinity.

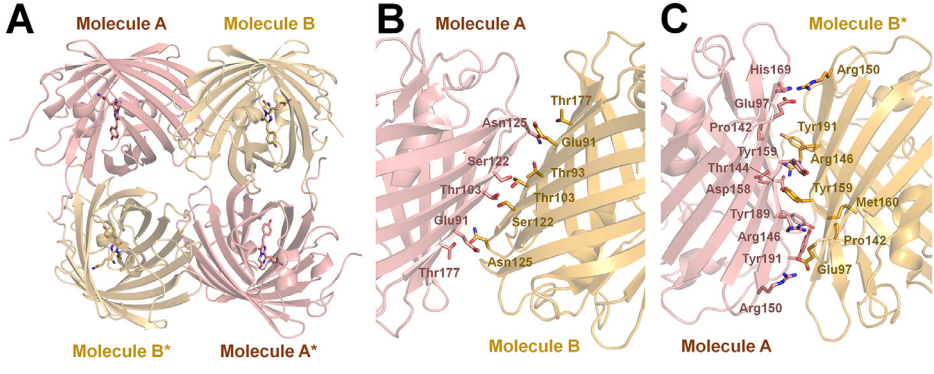

Fig. 4. Tetrameric structure of tKeima. (A) Tetrameric formation of tKeima. (B) Interaction of the A–B and A–B* interfaces in the tetrameric formation of tKeima.

Table 3
Molecular contacts of the A–B and A–B* interfaces in the tKeima tetramer.

Molecular contact of A-B interface in tKeima					
Molecule A [atom]	Distance (Å)	Molecule B [atom]	Molecule A [atom]	Distance (Å)	Molecule B [atom]
Asn20 [OD1]	3.43	Glu91 [OE1]	Ser122 [CB]	3.27	Thr103 [OG]
Asn20 [CA]	2.97	Glu91 [OE2]	Ser122 [OG]	2.77	Thr103 [OG]
Asn20 [C]	3.19	Glu91 [OE2]	Ser122 [CB]	3.32	Ser122 [CB]
Glu91 [OE2]	3.23	Asn20 [CA]	Asn125 [ND2]	3.31	Thr93 [OG1]
Glu91 [OE1]	2.91	Asn125 [N]	Asn125 [ND2]	3.49	Lys175 [CD]
Thr93 [CG2]	3.47	Val124 [CG2]	Asn125 [OD1]	3.50	Thr177 [OG1]
Thr103 [OG1]	2.57	Thr103 [OG]	Asn125 [OD1]	3.43	Glu91 [CB]
Thr103 [OG1]	3.32	Ser122 [CB]	Asn125 [N]	2.86	Glu91 [OE1]
Thr103 [CB]	3.47	Ser122 [OG]	Thr177 [CB]	3.49	Asn125 [OD1]
Thr103 [OG1]	2.65	Ser122 [OG]	Thr177 [OG1]	3.09	Asn125 [OD1]
Ser122 [OG]	3.42	Thr103 [CB]			
Molecular contact of A–B* interface in tKeima					
Molecule A [atom]	Distance (Å)	Molecule B* [atom]	Molecule A [atom]	Distance (Å)	Molecule B* [atom]
Glu97 [OE1]	2.98	Arg150 [NH1]	Asp158 [OD1]	3.18	Arg146 [NH1]
Glu97 [CD]	3.37	Arg150 [NH2]	Tyr159 [O]	3.46	Arg146 [CZ]
Glu97 [OE2]	2.72	Arg150 [NH2]	Tyr159 [O]	2.96	Arg146 [NH1]
Glu97 [OE1]	3.29	Arg150 [NH2]	Tyr159 [N]	3.38	Arg146 [NH2]
Glu141 [OE2]	3.23	Tyr189 [CB]	Tyr159 [CD2]	3.37	Tyr159 [CD2]
Glu141 [CB]	3.41	Tyr189 [CE2]	Tyr159 [OH]	2.91	Glu173 [CG]
Pro142 [O]	3.41	Tyr191 [CE1]	Tyr159 [OH]	3.06	Glu173 [CD]
Pro142 [O]	3.31	Tyr191 [CZ]	Tyr159 [OH]	2.92	Glu173 [OE2]
Pro142 [C]	3.43	Tyr191 [OH]	Ala161 [CB]	3.35	Tyr189 [CE1]
Pro142 [O]	2.53	Tyr191 [OH]	Ala161 [CB]	3.48	Tyr189 [CZ]
Pro142 [CB]	3.41	Tyr191 [OH]	Ala161 [CB]	3.49	Tyr189 [OH]
Thr144 [N]	3.29	Arg146 [NH1]	His169 [O]	3.05	Arg150 [NH2]
Thr144 [O]	3.06	Arg146 [NH2]	Glu173 [OE1]	3.41	Tyr159 [OH]
Arg146 [NH1]	3.37	Met160 [C]	Glu173 [OE2]	3.19	Glu173 [OE2]
Arg146 [CZ]	3.45	Met160 [O]	Tyr189 [CE2]	3.34	Ala161 [CB]
Arg146 [NH1]	2.78	Met160 [O]	Tyr191 [OH]	3.37	Pro142 [C]
Arg146 [NH2]	3.24	Met160 [O]	Tyr191 [OH]	2.33	Pro142 [O]
Arg146 [NH1]	3.48	Ala161 [CB]	Tyr191 [CZ]	3.31	Pro142 [O]
Phe148 [CZ]	3.46	Leu171 [CD1]	Asp193 [OD2]	3.38	Leu220 [CD1]
Arg150 [NH2]	2.78	His169 [O]	Ser219 [OG]	3.25	Pro142 [CB]
Arg150 [NH1]	3.15	Glu97 [OE1]	Ser219 [OG]	3.44	Pro142 [CG]
Arg150 [NH2]	2.95	Glu97 [OE2]	Leu220 [CD1]	3.47	Asp193 [OD2]
Asn157 [CB]	3.50	Tyr159 [CG]	Leu220 [CD1]	3.43	Leu220 [CD1]
Asn157 [CB]	3.30	Tyr159 [CD2]	Ile213 [CG2]	3.37	Leu221 [CD2]
Asn157 [CB]	3.37	Tyr159 [CE2]	Leu221 [O]	3.38	Lys195 [CD]
Asp158 [OD1]	3.46	Arg146 [NH2]			

raphy and analytical equilibrium ultracentrifugation [8]. At the A–B interface of tKeima, approximately 7.0 % of the surface area of each tKeima molecule was buried. The A–B interface is mainly stabilized by nine hydrogen bonds (Glu91–Asn125, Thr103–Thr103, Thr103–Ser122, Ser122–Thr103, Asn125–Glu91, Asn125–Thr93, Asn125–Thr177, and Thr177–Asn125; Fig. 4B). At the A–B* interface of tKeima, 12 % of the total monomer surface area was buried. The A–B* interface was stabilized by 14 hydrogen bonds

(molecules A–B*: Glu97–Arg150, Pro142–Tyr191, Thr144–Arg146, Arg146–Met160, Arg150–Glu97, Asp158–Arg146, Tyr159–Arg146, His169–Arg150, Tyr189–Tyr159, and Tyr191–Pro142) and seven salt-bridge interactions (Glu97–Arg150, Arg150–Glu97, and Asp158–Arg146; Fig. 4C). Thus, the tetrameric interfaces of tKeima are stabilized by hydrogen bonds and salt-bridge interactions. Analysis of the molecular contacts of the tKeima tetramer at distances below 3.5 Å showed that the A–B and A–B* interfaces exhibit 21 and 51 molecular contacts, respectively (Table 3).

4. Experimental Design, Materials and Methods

The DNA sequence of tKeima (UniProt: Q1JV72) was codon-optimized for expression in *Escherichia coli*. The codon-optimized tKeima sequence was synthesized by Bioneer (Daejeon, Republic of Korea). The synthetic tKeima gene was cloned into multiple cloning sites between the Nde site and the XhoI restriction site in the pET28a vector (Novagen). The DNA vector containing the tKeima gene was transformed into *E. coli* BL21 (DE3) competent cells (Novagen) using a heat-shock method at 42 °C. The cell containing pET28a with the tKeima gene was selected on an LB agar plate with 50 μL/mg kanamycin. Few colonies were cultured in 5 mL of LB broth medium containing 50 mg/mL kanamycin at 37 °C overnight. These culture cells were inoculated in 1 L of LB broth medium containing 50 mg/mL kanamycin on a shacking incubator at 180 rpm and 37 °C. When the optical density at 600 nm reached approximately 0.8, 0.5 mM isopropyl β-D-thiogalactopyranoside was added to induce protein expression and incubated in a shacking incubator at 18 °C for 18 h with shaking at 150 rpm. After harvesting the cells by centrifugation at 4000 rpm, the cell pellet was resuspended in a buffer containing 50 mM Tris–HCl (pH 8.0) and 200 mM NaCl. Cell lysis was performed on ice by sonication. After centrifugation at 13,000 rpm for 30 min, cell debris was removed. The supernatant was filtered using a 0.22-μm syringe filter and then loaded onto 5 mL of Ni-NTA resin (Qiagen) in a column. The resins were washed using a buffer containing 50 mM Tris–HCl (pH 8.0), 200 mM NaCl, and 20 mM imidazole. Proteins were eluted using a buffer containing 50 mM Tris–HCl (pH 8.0), 200 mM NaCl, and 300 mM imidazole. To remove the N-terminal hexahistidine tag, the thrombin was added into the protein solution and incubated at room temperature overnight. For size exclusion chromatography, the protein solution was concentrated using a concentrator (Merck Millipore) and then loaded onto a Sephacryl S-100 column (GE Healthcare) in a buffer containing 10 mM Tris–HCl (pH 8.0) and 200 mM NaCl. The tKeiam fractions were concentrated (~30 mg/mL) using a concentrator and stored at 4 °C overnight. The tKeima crystals were spontaneously grown without crystallization, which are used for X-ray diffraction at synchrotron. X-ray diffraction data were collected at the beamline 11C at PLS-II (Republic of Korea) [11]. A single rhombic-shaped tKeima crystal was fished using a nylon loop and cryoprotected using a solution containing 50 mM Tris–HCl (pH 8.0), 200 mM NaCl, and 20 % (v/v) glycerol for 10 s. The tKeima crystal was mounted on a goniometer under 100 K nitrogen stream. Diffraction data were recorded using a Pilatus 6 M detector (DECTRIS). The diffraction images were processed using the HKL2000 program [12]. Phasing problem was solved by molecular replacement method using the MOLREP [13] program and the crystal structure of dKeima570 (PDB ID: 8YDO) [14] as the search model. Model building of tKeima was performed using the COOT [15] program. Structure refinement was performed using the REFMAC5 [16] program implemented in CCP4 [17]. The model structure was validated using MolProbity [18]. The molecular contacts of the tetrameric interfaces of tKeima were analyzed using CCP4 [17].

Limitations

The determined crystal structure of tKeima was suitable for analyzing the overall architecture, the conformation of the chromophore, and the tetrameric assembly. However, the water molecules involved in the protonation/deprotonation of the chromophore were not clearly observed because the tKeima structure was determined at a medium resolution.

Ethics Statement

This work meets the ethical requirements for publication in this journal. This work does not involve human subjects, animal experiments, or any data collected from social media.

CRediT Author Statement

Ki Hyun Nam: Conceptualization, methodology, formal analysis, investigation, writing—original draft preparation, K.H.N.; **Yongbin Xu**: formal analysis, writing—review and editing, Y.X.

Data Availability

Crystal structure of large stokes shift red fluorescent protein tKeima (Original data) (Protein Data Bank)

Acknowledgments

We would like to thank the beamline staffs at the 11C beamline at the Pohang Light Source II for their assistance with data collection. This work was funded by the National Research Foundation of Korea (NRF) (NRF2021R1I1A1A01050838 to K.H.N.). This work was supported by Fundamental Research Funds for the Central Universities (grant No 04442024017 to Y.X.).

Declaration of Competing Interest

The authors declare that they have no known competing financial interests or personal relationships that could have appeared to influence the work reported in this paper.

References

[1] K.H. Nam, Y. Xu, Structural analysis of the large stokes shift red fluorescent protein tKeima, Molecules 29 (2024) 2579, doi:10.3390/molecules29112579.
[2] M. Zimmer, Green fluorescent protein (GFP): applications, structure, and related photophysical behavior, Chem. Rev. 102 (2002) 759–782, doi:10.1021/cr010142r.
[3] D.M. Chudakov, M.V. Matz, S. Lukyanov, K.A. Lukyanov, Fluorescent proteins and their applications in imaging living cells and tissues, Physiol. Rev. 90 (2010) 1103–1163, doi:10.1152/physrev.00038.2009.
[4] I.J. Kim, S. Kim, J. Park, I. Eom, S. Kim, J.H. Kim, S.C. Ha, Y.G. Kim, K.Y. Hwang, K.H. Nam, Crystal structures of Dronpa complexed with quenchable metal ions provide insight into metal biosensor development, FEBS Lett. 590 (2016) 2982–2990, doi:10.1002/1873-3468.12316.
[5] I.J. Kim, Y. Xu, K.H. Nam, Metal-induced fluorescence quenching of photoconvertible fluorescent protein DendFP, Molecules 27 (2022) 2922, doi:10.3390/molecules27092922.
[6] K.H. Nam, Fluorescent protein-based metal biosensors, Chemosensors 11 (2023) 216, doi:10.3390/chemosensors11040216.
[7] T. Kogure, H. Kawano, Y. Abe, A. Miyawaki, Fluorescence imaging using a fluorescent protein with a large Stokes shift, Methods 45 (2008) 223–226, doi:10.1016/j.ymeth.2008.06.009.
[8] T. Kogure, S. Karasawa, T. Araki, K. Saito, M. Kinjo, A. Miyawaki, A fluorescent variant of a protein from the stony coral Montipora facilitates dual-color single-laser fluorescence cross-correlation spectroscopy, Nat. Biotechnol. 24 (2006) 577–581, doi:10.1038/nbt1207.
[9] R.N. Day, M.W. Davidson, The fluorescent protein palette: tools for cellular imaging, Chem. Soc. Rev. 38 (2009) 2887, doi:10.1039/b901966a.
[10] T.M. Wannier, S.K. Gillespie, N. Hutchins, R.S. McIsaac, S.-Y. Wu, Y. Shen, R.E. Campbell, K.S. Brown, S.L. Mayo, Monomerization of far-red fluorescent proteins, Proc. Natl. Acad. Sci. U.S.A. 115 (2018) E11294–E11301, doi:10.1073/pnas.1807449115.
[11] D.H. Gu, C. Eo, S.A. Hwangbo, S.C. Ha, J.H. Kim, H. Kim, C.S. Lee, I.D. Seo, Y.D. Yun, W. Lee, et al., BL-11C Micro-MX: a high-flux microfocus macromolecular-crystallography beamline for micrometre-sized protein crystals at Pohang Light Source II, J. Synchrotron Radiat. 28 (2021) 1210–1215, doi:10.1107/S1600577521004355.
[12] Z. Otwinowski, W. Minor, Processing of X-ray diffraction data collected in oscillation mode, Methods Enzymol. 276 (1997) 307–326, doi:10.1016/S0076-6879(97)76066-X.
[13] A. Vagin, A. Teplyakov, Molecular replacement with MOLREP, Acta Crystallogr. D Biol. Crystallogr. 66 (2010) 22–25, doi:10.1107/S0907444909042589.
[14] Y. Xu, K.Y. Hwang, K.H. Nam, Spectral and structural analysis of large Stokes shift fluorescent protein dKeima570, J. Microbiol. 56 (2018) 822–827, doi:10.1007/s12275-018-8319-5.
[15] A. Casañal, B. Lohkamp, P. Emsley, Current developments in coot for macromolecular model building of electron cryo-microscopy and crystallographic data, Protein Sci. 29 (2020) 1055–1064, doi:10.1002/pro.3791.

[16] G.N. Murshudov, P. Skubak, A.A. Lebedev, N.S. Pannu, R.A. Steiner, R.A. Nicholls, M.D. Winn, F. Long, Vagin, A.A. REFMAC5 for the refinement of macromolecular crystal structures, Acta Crystallogr. D Biol. Crystallogr. 67 (2011) 355–367, doi:10.1107/S0907444911001314.
[17] J. Agirre, M. Atanasova, H. Bagdonas, C.B. Ballard, A. Baslé, J. Beilsten-Edmands, R.J. Borges, D.G. Brown, J.J. Burgos-Mármol, J.M. Berrisford, et al., The CCP4 suite: integrative software for macromolecular crystallography, Acta Crystallogr. D Biol. Crystallogr 79 (2023) 449–461, doi:10.1107/s2059798323003595.
[18] C.J. Williams, J.J. Headd, N.W. Moriarty, M.G. Prisant, L.L. Videau, L.N. Deis, V. Verma, D.A. Keedy, B.J. Hintze, V.B. Chen, et al., MolProbity: more and better reference data for improved all-atom structure validation, Protein Sci 27 (2018) 293–315, doi:10.1002/pro.3330.